Acknowledgments

We thank Y. Mizutani and R. Varillas for excellent technical help. We thank V. Campuzano and M. Barbacid for the RERTert mouse line and M. Endoh for the *Eomes* primers and help with the ChIP experiments. T.E. acknowledges Dr. Toyoda's support. M.R-T. and H. M-G. were recipients of FPU and FPI fellowships, respectively, from the Ministerio de Educacion y Ciencia and Comunidad de Madrid, respectively. This work was supported by grants SAF2007-65957-C02-01 (M.V.), the Onco-Cycle program from the Comunidad de Madrid (M.V.), SAF2004-05798, and CIBERNED CB06/05/0065 from Instituto de Salud Carlos III (C.V-A.)

Disclosure of Potential Conflicts of Interest

The authors indicate no potential conflicts of interest.

References

1 Weissman IL. Stem cells: Units of development, units of regeneration, and units in evolution. Cell 2000;100:157–168.
2 Morrison SJ, Kimble J. Asymmetric and symmetric stem-cell divisions in development and cancer. Nature 2006;441:1068–1074.
3 Molofsky AV, Pardal R, Morrison SJ. Diverse mechanisms regulate stem cell self-renewal. Curr Opin Cell Biol 2004;16:700–707.
4 Orford KW, Scadden DT. Deconstructing stem cell self-renewal: Genetic insights into cell-cycle regulation. Nat Rev Genet 2008;9: 115–128.
5 Mimeault M, Batra SK. Concise review: Recent advances on the significance of stem cells in tissue regeneration and cancer therapies. Stem Cells 2006;24:2319–2345.
6 Kim J, Chu J, Shen X et al. An extended transcriptional network for pluripotency of embryonic stem cells. Cell 2008;132:1049–1061.
7 Niwa H. How is pluripotency determined and maintained? Development 2007;134:635–646.
8 Silva J, Smith A. Capturing pluripotency. Cell 2008;132:532–536.
9 Spivakov M, Fisher AG. Epigenetic signatures of stem-cell identity. Nat Rev Genet 2007;8:263–271.
10 Cao R, Wang L, Wang H et al. Role of histone H3 lysine 27 methylation in Polycomb-group silencing. Science 2002;298:1039–1043.
11 Wang H, Wang L, Erdjument-Bromage H et al. Role of histone H2A ubiquitination in Polycomb silencing. Nature 2004;431:873–878.
12 Levine SS, King IF, Kingston RE. Division of labor in Polycomb group repression. Trends Biochem Sci 2004;29:478–485.
13 Boyer LA, Plath K, Zeitlinger J et al. Polycomb complexes repress developmental regulators in murine embryonic stem cells. Nature 2006;441:349–353.
14 Bracken AP, Dietrich N, Pasini D et al. Genome-wide mapping of Polycomb target genes unravels their roles in cell fate transitions. Genes Dev 2006;20:1123–1136.
15 Lee TI, Jenner RG, Boyer LA et al. Control of developmental regulators by Polycomb in human embryonic stem cells. Cell 2006;125: 301–313.
16 Stock JK, Giadrossi S, Casanova M et al. Ring1-mediated ubiquitination of H2A restrains poised RNA polymerase II at bivalent genes in mouse ES cells. Nat Cell Biol 2007;9:1428–1435.
17 Wang L, Brown JL, Cao R et al. Hierarchical recruitment of Polycomb group silencing complexes. Mol Cell 2004;14:637–646.
18 Cao R, Tsukada YI, Zhang Y. Role of Bmi-1 and Ring1A in H2A ubiquitylation and Hox gene silencing. Mol Cell 2005;20:845–854.
19 Schoeftner S, Sengupta AK, Kubicek S et al. Recruitment of PRC1 function at the initiation of X inactivation independent of PRC2 and silencing. EMBO J 2006;25:3110–3122.
20 Valk-Lingbeek ME, Bruggeman SW, Van Lohuizen M. Stem cells and cancer: the Polycomb connection. Cell 2004;118:409–418.
21 Mohn F, Weber M, Rebhan M et al. Lineage-specific Polycomb targets and de novo DNA methylation define restriction and potential of neuronal progenitors. Mol Cell 2008;30:755–766.
22 Li Z, Cao R, Wang M et al. Structure of a Bmi-1-Ring1B Polycomb group ubiquitin ligase complex. J Biol Chem 2006;281:20643–20649.
23 Bruggeman SW, Valk-Lingbeek ME, van der Stoop PP et al. Ink4a and Arf differentially affect cell proliferation and neural stem cell self-renewal in Bmi1-deficient mice. Genes Dev 2005;19:1438–1443.
24 Molofsky AV, Pardal R, Iwashita T et al. Bmi-1 dependence distinguishes neural stem cell self-renewal from progenitor proliferation. Nature 2003;425:962–967.
25 Molofsky AV, He S, Bydon M et al. Bmi-1 promotes neural stem cell self-renewal and neural development but not mouse growth and survival by repressing the p16Ink4a and p19Arf senescence pathways. Genes Dev 2005;19:1432–1437.
26 Fasano CA, Dimos JT, Ivanova NB et al. shRNA knockdown of Bmi-1 reveals a critical role for p21-Rb pathway in NSC self-renewal during development. Cell Stem Cell 2007;1:87–99.
27 Buchwald G, van der Stoop P, Weichenrieder O et al. Structure and E3-ligase activity of the Ring-Ring complex of Polycomb proteins Bmi1 and Ring1b. EMBO J 2006;25:2465–2474.
28 Calés C, Román-Trufero M, Pavón L et al. Inactivation of the Polycomb group protein Ring1B unveils an antiproliferative role in hematopoietic cell expansion and cooperation with tumorigenesis associated with Ink4a deletion. Mol Cell Biol 2008;28:1018–1028.
29 del Mar Lorente M, Marcos-Gutiérrez C, Pérez C et al. Loss- and gain-of-function mutations show a Polycomb group function for Ring1A in mice. Development 2000;127:5093–5100.
30 Mijimolle N, Velasco J, Dubus P et al. Protein farnesyltransferase in embryogenesis, adult homeostasis, and tumor development. Cancer Cell 2005;7:313–324.
31 Seibler J, Zevnik B, Küter-Luks B et al. Rapid generation of inducible mouse mutants. Nucleic Acids Res 2003;31:e12.
32 Vergaño-Vera E, Yusta-Boyo MJ, de Castro F et al. Generation of GABAergic and dopaminergic interneurons from endogenous embryonic olfactory bulb precursor cells. Development 2006;133: 4367–4379.
33 Vicario-Abejón C, Yusta-Boyo MJ, Fernández-Moreno C et al. Locally born olfactory bulb stem cells proliferate in response to insulin-related factors and require endogenous insulin-like growth factor-I for differentiation into neurons and glia. J Neurosci 2003;23: 895–906.
34 García E, Marcos-Gutiérrez C, del Mar Lorente M et al. RYBP, a new repressor protein that interacts with components of the mammalian Polycomb complex, and with the transcription factor YY1. EMBO J 1999;18:3404–3418.
35 Wu Z, Irizarry R, Gentleman R et al. A model-based background adjustment for oligonucleotide expression arrays. J Am Stat Assoc 2004;99:909–917.
36 Hijikata A, Kitamura H, Kimura Y et al. Construction of an open-access database that integrates cross-reference information from the transcriptome and proteome of immune cells. Bioinformatics 2007; 23:2934–2941.
37 Draghici S, Khatri P, Martins RP et al. Global functional profiling of gene expression. Genomics 2003;81:98–104.
38 Benjamini Y, Hochberg Y. Controlling the false discovery rate: A practical and powerful approach to multiple testing. J R Stat Soc Ser B Methodol 1995;57:289–300.
39 Wang X, Seed B. A PCR primer bank for quantitative gene expression analysis. Nucleic Acids Res 2003;31:e154.
40 Reynolds BA, Rietze RL. Neural stem cells and neurospheres—re-evaluating the relationship. Nat Methods 2005;2:333–336.
41 Gritti A, Bonfanti L, Doetsch F et al. Multipotent neural stem cells reside into the rostral extension and olfactory bulb of adult rodents. J Neurosci 2002;22:437–445.
42 Voncken JW, Roelen BA, Roefs M et al. Rnf2 (Ring1b) deficiency causes gastrulation arrest and cell cycle inhibition. Proc Natl Acad Sci U S A 2003;100:2468–2473.
43 Indra AK, Warot X, Brocard J et al. Temporally-controlled site-specific mutagenesis in the basal layer of the epidermis: Comparison of the recombinase activity of the tamoxifen-inducible Cre-ER(T) and Cre-ER(T2) recombinases. Nucleic Acids Res 1999;27:4324–4327.
44 Endoh M, Endo TA, Endoh T et al. Polycomb group proteins Ring1A/B are functionally linked to the core transcriptional regulatory circuitry to maintain ES cell identity. Development 2008;135: 1513–1524.
45 Seo S, Lim J, Yellajoshyula D et al. Neurogenin and NeuroD direct transcriptional targets and their regulatory enhancers. EMBO J 2007; 26:5093–5108.
46 Hitoshi S, Alexson T, Tropepe V et al. Notch pathway molecules are essential for the maintenance, but not the generation, of mammalian neural stem cells. Genes Dev 2002;16:846–858.
47 Ohtsuka T, Sakamoto M, Guillemot F et al. Roles of the basic helix-loop-helix genes Hes1 and Hes5 in expansion of neural stem cells of the developing brain. J Biol Chem 2001;276: 30467–30474.

48 Sherr CJ, Roberts JM. CDK inhibitors: Positive and negative regulators of G1-phase progression. Genes Dev 1999;13:1501–1512.
49 Molofsky AV, Slutsky SG, Joseph NM et al. Increasing p16INK4a expression decreases forebrain progenitors and neurogenesis during ageing. Nature 2006;443:448–452.
50 Kippin TE, Martens DJ, Kooy DVD. p21 loss compromises the relative quiescence of forebrain stem cell proliferation leading to exhaustion of their proliferation capacity. Genes Dev 2005;19:756–767.
51 Meletis K, Wirta V, Hede S et al. p53 suppresses the self-renewal of adult neural stem cells. Development 2006;133:363–369.
52 Smukler SR, Runciman SB, Xu S et al. Embryonic stem cells assume a primitive neural stem cell fate in the absence of extrinsic influences. J Cell Biol 2006;172:79–90.
53 Tropepe V, Hitoshi S, Sirard C et al. Direct neural fate specification from embryonic stem cells: A primitive mammalian neural stem cell stage acquired through a default mechanism. Neuron 2001;30:65–78.
54 Leeb M, Wutz A. Ring1B is crucial for the regulation of developmental control genes and PRC1 proteins but not X inactivation in embryonic cells. J Cell Biol 2007;178:219–229.
55 de la Pompa JL, Wakeham A, Correia KM et al. Conservation of the Notch signalling pathway in mammalian neurogenesis. Development 1997;124:1139–1148.
56 Bertrand N, Castro DS, Guillemot F. Proneural genes and the specification of neural cell types. Nat Rev Neurosci 2002;3:517–530.
57 Kageyama R, Ohtsuka T, Hatakeyama J et al. Roles of bHLH genes in neural stem cell differentiation. Exp Cell Res 2005;306:343–348.
58 Ross SE, Greenberg ME, Stiles CD. Basic helix-loop-helix factors in cortical development. Neuron 2003;39:13–25.
59 Yoon K, Gaiano N. Notch signaling in the mammalian central nervous system: Insights from mouse mutants. Nat Neurosci 2005;8:709–715.
60 Perissi V, Scafoglio C, Zhang J, Ohgi KA, Rose DW, Glass CK, Rosenfeld MG. TBL1 and TBLR1 phosphorylation on regulated gene promoters overcomes dual CtBP and NCoR/SMRT transcriptional repression checkpoints. Mol Cell 2008;29:755–766.
61 Sánchez C, Sánchez I, Demmers JA et al. Proteomic analysis of Ring1B/Rnf2 interactors identifies a novel complex with the Fbx110/Jhdm1B histone demethylase and the Bcl6 interacting corepressor. Mol Cell Proteomics 2007;6:820–834.
62 Elderkin S, Maertens GN, Endoh M et al. A phosphorylated form of Mel-18 targets the Ring1B histone H2A ubiquitin ligase to chromatin. Mol Cell 2007;28:107–120.
63 Rangarajan A, Talora C, Okuyama R et al. Notch signaling is a direct determinant of keratinocyte growth arrest and entry into differentiation. EMBO J 2001;20:3427–3436.
64 Radtke F, Raj K. The role of Notch in tumorigenesis: Oncogene or tumour suppressor? Nat Rev Cancer 2003;3:756–767.
65 Calegari F, Huttner WB. An inhibition of cyclin-dependent kinases that lengthens, but does not arrest, neuroepithelial cell cycle induces premature neurogenesis. J Cell Sci 2003;116:4947–4955.
66 Vanderluit JL, Wylie CA, McClellan KA et al. The retinoblastoma family member p107 regulates the rate of progenitor commitment to a neuronal fate. J Cell Biol 2007;178:129–139.
67 Sher F, Rössler R, Brouwer N et al. Differentiation of neural stem cells into oligodendrocytes: Involvement of the Polycomb group protein Ezh2. Stem Cells 2008;26:2875–2883.

See www.StemCells.com for supporting information available online.

Maintenance of Undifferentiated State and Self-Renewal of Embryonic Neural Stem Cells by Polycomb Protein Ring1B

Mónica Román-Trufero, Héctor R. Méndez-Gómez, Claudia Pérez, Atsushi Hijikata, Yu-ichi Fujimura, Takaho Endo, Haruhiko Koseki, Carlos Vicario-Abejón and Miguel Vidal

Stem Cells 2009;27;1559-1570
DOI: 10.1002/stem.82

Biochemical and Biophysical Research Communications 392 (2010) 252–257

Contents lists available at ScienceDirect

Biochemical and Biophysical Research Communications

journal homepage: www.elsevier.com/locate/ybbrc

LMO3 interacts with p53 and inhibits its transcriptional activity

Steven Larsen, Tomoki Yokochi, Eriko Isogai, Yohko Nakamura, Toshinori Ozaki, Akira Nakagawara *

Division of Biochemistry and Innovative Cancer Therapeutics, Chiba Cancer Center Research Institute, Chiba, Japan

ARTICLE INFO

Article history:
Received 1 December 2009
Available online 6 December 2009

Keywords:
LMO3
p53
LIM-only protein
Tumor suppressor
Oncogene
Neuroblastoma

ABSTRACT

High expression of LMO3 contributes to the development and aggressiveness of neuroblastoma. LMO3 belongs to the LIM-only protein family, in which de-regulation of its members is implicated in human carcinogenesis. However, the molecular mechanism of LMO3 activity in oncogenesis remained poorly characterized. We found that LMO3 is a direct interacting partner of p53 both *in vitro* and *in vivo*. The DNA-binding domain of p53 is required for this interaction. Furthermore, expression of LMO3 repressed p53-dependent mRNA expression of its target genes by suppressing promoter activation. Interestingly, chromatin immunoprecipitation assay showed that LMO3 facilitated p53 binding to its response elements. This suggests that LMO3 acts as a co-repressor of p53, suppressing p53-dependent transcriptional regulation without inhibition of its DNA-binding activity.

Introduction

Cancer is predominantly a genetic disease. Alterations in genes controlling cell growth, survival and apoptosis are most commonly implicated in carcinogenesis. Our knowledge of cancer biology and medicine is currently increasing at an exponential rate, yet the transition to clinical applications is progressing much slower. Therefore, new targets and pathways need to be identified, particularly those having clinical significance and with the potential for specific and novel therapeutic applications at the bedside. Neuroblastoma is one of the most common childhood cancers and is originated from sympathoadrenal lineage of the neural crest [1]. The bulk of sporadic neuroblastomas are detected at advanced stage with poor survival rates of less than 40%, despite intensive multimode therapy [2]. Often, initial therapy appears effective but is frequently followed by the appearance of drug resistance, with frequent acquisition of p53-mutations.

The tumor suppressor p53 is one of the key tumor suppressors protecting against cancer and genetic abnormalities, with mutations in over half of all human cancers [3]. In fact, the bulk of p53 mutations occur in the DNA-binding domain affecting the ability of p53 to act as an effective transcription factor [4]. High levels of *p53* mRNA are described for neuroblastoma cell lines, yet p53 mutations are reported in less than 2% of neuroblastomas compared with up to 60% in other cancers. p53 is thought to be inactivated by alternative mechanisms. In fact, the subject of p53 inactivation is one of the most controversial topics in neuroblastoma research [5].

The nuclear LIM-only proteins consist of four members, LMO1, LMO2, LMO3, and LMO4. They are twin LIM-domain containing proteins that mediate protein–protein interactions, which can bind to transcription factors forming a DNA-binding complex. Despite strong links with transcriptional regulation, no DNA-binding activity has been found. They demonstrated decisive roles in distinct developmental pathways and that de-regulation of their expression is linked to oncogenesis [6–8]. De-regulation of LIM-only protein family members have been implicated in various cancers. Transgenic mice for the founding members, LMO1 and LMO2, developed immature and aggressive T-cell leukemia [9]. The more recently discovered LMO-family member, LMO4, is implicated in the cause and progression of human breast cancers [10], sqaumous cell carcinomas of the oral cavity [11] and primary prostate cancers [12]. LMO3 binding to its interacting partners is involved in cell fate determination of the sympathoadrenal lineage and is closely related to development of neuroblastoma [6,13,14]. Double knockout mice for *LMO1* and *LMO3* demonstrated a lethal phenotype [6]. Bao et al. [13] reported the cooperation of *Xenopus* HEN1 with XLMO3 as a critical regulator of neurogenesis. In the case of LMO1, the LIM domain shares 98% homology with LMO3 [6,14,15] and demonstrates redundancy in murine *in vivo* studies, in which double mutants of *LMO1* and *LMO3* transgenic mice exhibited perinatal death. Whereas, single mutants of either of these genes developed with an apparently normal phenotype [6]. Additionally, several oncogenic characteristics arising from LMO3 expression have been identified, both *in vitro* and *in vivo*. These include increased cell proliferation in normal and low serum conditions, colony formation in soft agar and rapid tumor growth in

* Corresponding author. Address: Division of Biochemistry and Innovative Cancer Therapeutics, Chiba Cancer Center Research Institute, 666-2 Nitona, Chuou-ku, Chiba 260-8717, Japan. Fax: +81 43 265 4459.
E-mail address: akiranak@chiba-cc.jp (A. Nakagawara).

0006-291X/$ - see front matter © 2009 Elsevier Inc. All rights reserved.
doi:10.1016/j.bbrc.2009.12.010

nude mice of SH-SY5Y cells stably expressing LMO3 [14]. High levels of *LMO3* mRNA were found in aggressive neuroblastomas with a poor prognosis as compared with more favorable subtypes [14]. In our previous report, analysis of cDNA libraries from different subsets of neuroblastoma and cloning of 4200 genes identified *LMO3* as being differentially expressed in neuroblastoma [15]. Clinical studies revealed that low expression of *LMO3* correlated with a favorable probability of survival and high expression with a much poorer prognosis [14].

The molecular mechanisms of LMO3 activity in oncogenesis remain poorly characterized and the potential for inhibition of tumor suppressors has not been investigated to date. The novel finding presented here is that LMO3 can function as an oncogene by binding to and inhibiting the key tumor suppressor p53, which results in reduced transcription of apoptosis-related genes.

Materials and methods

Cell lines and transfection assays. Small cell lung carcinoma, H1299 and African green monkey, COS-7 mammalian cells were maintained at 37 °C/5% CO_2 in either RPMI 1640 or DMEM supplemented with 10% heat inactivated fetal bovine serum, 100 IU/ml penicillin and 100 μg/ml streptomycin. Where indicated, cells were transfected using either LipofectAMINE 2000 (Invitrogen, CA, USA) or FuGene HD (Roche Applied Science, IN, USA) transfection reagents according to manufacturer recommendations. Total amount of transfected plasmid DNA was adjusted to constant levels with empty parental pcDNA3 plasmid (Invitrogen).

Immunoprecipitation and GST-pull down assays. Immunoprecipitation was essentially performed as in [16] using anti-p53 (DO-1, Calbiochem, CA, USA; pab1801, Santa Cruz Biotechnology, CA, USA) monoclonal antibodies; or anti-flag tag (M2; Sigma, MI, USA) monoclonal antibody. Immunoprecipitated proteins were resolved by SDS–PAGE and detected by immunoblotting.

For the *in vitro* GST-pull down experiments, plasmid constructs encoding the p53 deletion mutants, p53 (1–359), p53 (1–292), p53 (1–102) and p53 (102–393) were used to create the respective [^{35}S]-methionine labeled proteins by an *in vitro* coupled transcription/translation system (Promega, WI, USA). GST only or GST-LMO3 fusion protein was produced by induction with isopropyl β-D-1-thiogalactopyranoside (IPTG) and expression in bacteria and purified with Glutathione Sepharose beads. Expression efficiency and purification was checked by Coomassie Brilliant Blue R-250 (CBB) staining and western blot analysis. Approximately equimolar amounts (determined by SDS–PAGE) of GST or GST-LMO3 fusion proteins were immobilized on glutathione-Sepharose beads and incubated with *in vitro* translated p53 deletion mutants, essentially as described in [17]. The bound [^{35}S]-methionine labeled proteins were resolved by 12% SDS–PAGE, incubation with Amplify (Amersham, Chalfont, UK) enhancer reagent and detected by autoradiography.

Semi-quantitative RT-PCR. Total RNA was isolated and purified from cultured cells using the RNeasy kit (Qiagen, Hilden, Germany). The RNA concentration was calculated and equal amounts were reverse transcribed using SuperScript II reverse transcriptase and random primers (Invitrogen). The resultant cDNA was subject to PCR-based amplification with gene-specific primers (sequences are available on request).

Indirect immunofluorescence. H1299 cells were grown on sterile coverslips 1 day prior to transfection with p53 and FLAG-LMO3 expression constructs, then slides prepared for immunofluorescence microscopy as described in [18]. Cells were incubated with a mixture of polyclonal anti-FLAG epitope and monoclonal anti-p53 (DO-1; Calbiochem) primary antibodies and fluorescein isothiocyanate- (FITC) or Rhodamine-conjugated secondary antibodies. Cover slips were mounted onto glass slides using 4,6-diamidino-2-phenylindole dihydrochloride (DAPI) containing Vector Shield mounting medium (Vector Laboratories, CA, USA) and imaged using fluorescence microscopy and Image Ready Easy software.

Luciferase gene reporter assay. H1299 cells plated in a 12-well plate were allowed to adhere overnight and then transfected with indicated reporter constructs and *Renilla* luciferase by Lipofect-AMINE 2000 (Invitrogen). Total amount of transfected DNA was kept constant with empty pcDNA3 plasmid. Both *Renilla* and firefly luciferase activity were assayed at 36 h post-transfection using the dual-luciferase reporter assay system (Promega). Firefly gene reporter activity was calculated relative to *Renilla* luminescence.

Chromatin immunoprecipitation. Chromatin immunoprecipitation assays were performed using reagents and the protocol provided by Upstate Biotechnology (NY, USA), with the modification that purification of de-crosslinked DNA was performed using QIAquick PCR purification kit (Qiagen). Purified DNA was analyzed by PCR-based amplification of p53 responsive elements of *p21*, *bax*, and *puma* promoters using the specific primers as follows: *p21*, 5′-gagcctccctccatccctat-3′ (forward), 5′-ctgctgcccaagcatgttc-3′ (reverse); *bax*, 5′-cggtagctcatgcctgtaatcc-3′ (forward), 5′-aacttgtgagcc-caagagataacc-3′ (reverse); *puma*, 5′-gccttgtgtctgtgagtacatcct-3′ (forward), 5′-gttccagggtccacaaagtca-3′ (reverse).

Immunoblotting and antibodies. Equivalent amounts of protein lysates normalized to actin levels were separated by SDS–PAGE, transferred to a polyvinylidene fluoride membrane (Millipore, MA, USA). The membrane was probed with anti-p53 (DO-1; Calbiochem), anti-phospho ser 15 p53 (Cell Signalling Technology, MA, USA) anti-FLAG tag (M2; Sigma), anti-HA tag (6E2; Cell Signalling Technology), anti-actin (Sigma), anti-PARP (Cell Signalling Technology) antibody followed by incubation with horseradish peroxidase conjugated goat anti-mouse or anti-rabbit secondary antibody (Cell Signalling Technology). Immunoblots were visualized by enhanced chemoluminescence reagents (Amersham) and exposed to X-ray film.

Results

Physical interaction between LMO3 and the DNA-binding domain of p53

LMO3 was previously described as an oncogene in neuroblastoma [14] and mutations of p53 are rarely found in this childhood cancer. However, the p53 tumor suppressor is thought to be inactivated by alternative pathways. Furthermore, binding to and inhibition of tumor suppressors are reported for other LIM-only protein family members. Additionally, LIM-only proteins are involved in protein–protein interactions and known to act as cofactors in DNA-binding complexes. Considering these facts, we examined a potential relationship between LMO3 and the p53 pathway. Towards this aim, we used indirect immunofluorescence to identify the subcellular distributions of LMO3 and p53 (Fig. 1A). LMO3 protein (green) was predominantly localized in the cell nucleus (blue), indicating that LMO3 is principally a nuclear protein when expressed in p53-null H1299 cells. Merged images of LMO3 and p53 (red) staining revealed co-localization in the cell nucleus. These observations suggested a possible association of LMO3 with p53 in the cell nucleus.

Leading on from the co-localization experiments, *in vitro* and *in vivo* binding studies were performed (Fig. 1B–1E). Cell lysates prepared from H1299 cells co-transfected with p53 and LMO3 were subjected to immunoprecipitation with either an anti-FLAG (1B; left panel) or an anti-p53 (Fig. 1B; right panel). Immunoprecipitated proteins were detected by immunoblotting with anti-p53 and anti-FLAG antibodies, respectively. This suggests that

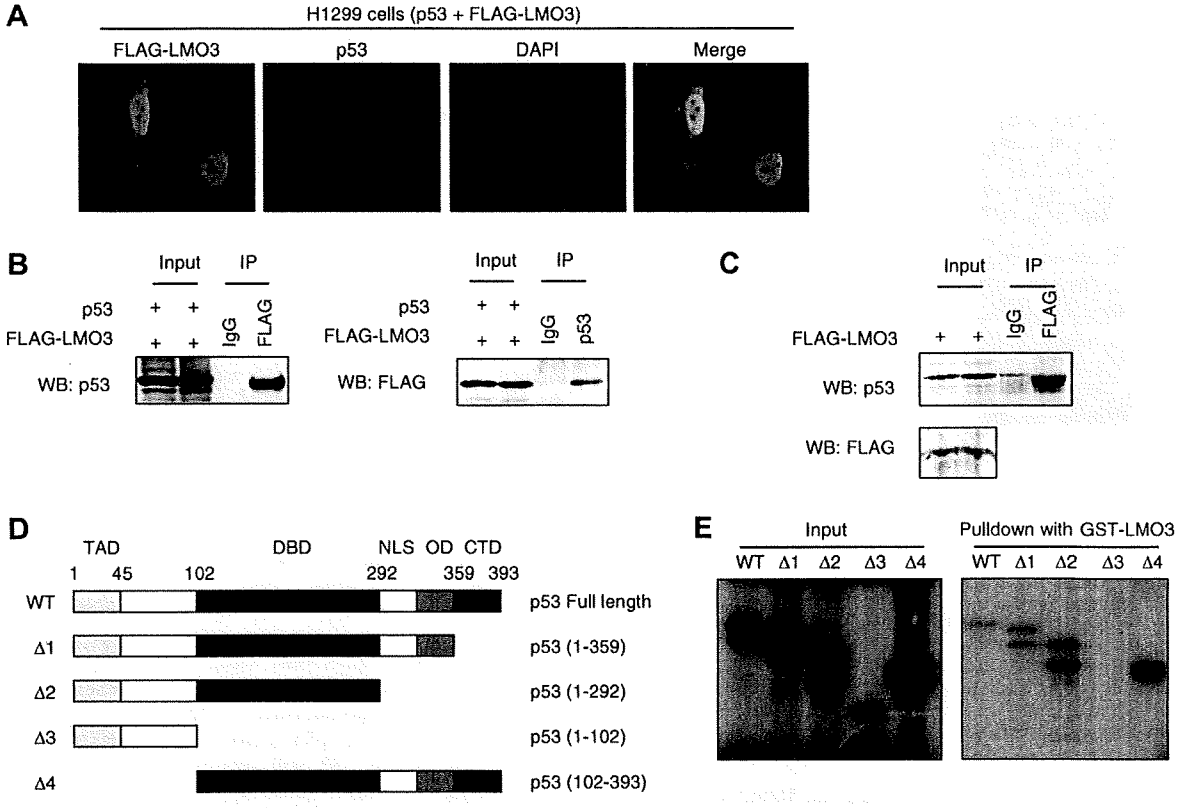

Fig. 1. Direct physical interaction of p53 and LMO3, requiring the DNA-binding domain of p53. (A) Co-localization of p53 and LMO3 in H1299 cells by indirect-immunofluorescence. Cells were transfected with p53 and FLAG-LMO3 expression vectors, and then incubated with a combination of anti-p53 (red) and polyclonal anti-FLAG (green) antibodies. The nuclei were visualized by DAPI staining (blue). (B) Either anti-FLAG (left panel) or anti-p53 (right panel) antibodies were used to prepare immunoprecipitates from H1299 cells co-transfected with p53 and FLAG-LMO3. These cells were treated with 10 μM MG132 8 h prior to harvest. Co-immunoprecipitated proteins were analyzed by western blotting. (C) Co-immunoprecipitation of endogenous p53 with FLAG-LMO3 antibody. (D) Schematic representation of p53 domain structures and deletion mutants used in this study. Amino acid residues are indicated by numbers. TAD, transactivation domain; DBD, DNA-binding domain; NLS, nuclear localization; OD, oligomerization domain; CTD, C-terminal regulatory domain. (E) p53 binding domain determination by *in vitro* GST-pull down assay. *In vitro* binding assay using translated ^{35}S labeled full length and deletion mutants of p53 are shown; input (left panel); pulldown with GST-LMO3 (right panel).

p53 and LMO3 proteins can physically interact, indicating the capacity of LMO3 to form a stable association with p53 in cells.

To confirm the binding of LMO3 with endogenous p53, whole cell lysate prepared from COS-7 cells transfected with FLAG-LMO3 was immunoprecipitated with anti-FLAG antibody (Fig. 1C) and then immunoblotted with anti-p53 antibody. Immunocomplexes containing endogenous p53 protein could be detected in anti-FLAG antibody immunoprecipitates for COS-7 cells expressing FLAG-tagged LMO3. Immunoprecipitation of cell lysates with normal mouse IgG did not contain LMO3 or p53. In these experiments, LMO3 could co-immunoprecipitate with p53, demonstrating a physical interaction between these two proteins in cells.

To examine this physical interaction in detail, we determined the essential region(s) of p53 responsible for this interaction. We carried out *in vitro* binding studies using recombinant p53 proteins constructed with a series of deletions [16], depicted in Fig. 1D. These constructs contain deletion of the C-terminal regulatory domain (CTD), nuclear localization domain (NLS), oligomerization domain (OD), DNA-binding domain (DBD) or transcriptionally active domain (TAD). The GST-LMO3 bead complex was incubated with radiolabeled p53 deletion mutants, generated by an *in vitro* transcription/translation system in the presence of [^{35}S]-methionine (Fig. 1E; left panel). GST-LMO3 could pull down all of the p53 deletion mutants, with the exception of p53 (1–102). This result implies that the region between amino acid residues 102 and 292 of p53 (DBD) is required for the physical interaction with LMO3 (Fig. 1E; right panel), suggesting that LMO3 directly binds to the DNA-binding domain of p53.

LMO3 demonstrates repressor activity on p53-mediated transcriptional activation

The functional significance of this LMO3-p53 interaction was investigated by assessing the ability of p53 to activate its target gene expression. Detection of endogenous mRNAs by RT-PCR was used to assess the effect of LMO3 expression on the transcriptional ability of p53 (Fig. 2A). H1299, a p53-null cell line, was co-transfected with constant amount of p53 expression plasmid and increasing amount of LMO3 plasmid. Expression of LMO3 repressed p53-mediated induction of its target genes, such as $p21^{WAF1}$, *Noxa*, *Bax*, and *Puma*. Endogenous mRNAs were repressed in a dose-dependent manner by co-expression of LMO3 (Fig. 2A). Constant expression of p53 and dose dependent expression of LMO3 were confirmed by RT-PCR. To further confirm this transcriptional repression, we utilized a firefly/*Renilla* luciferase gene reporter assay to analyze promoter activation of p53 target genes. Luciferase gene reporter constructs possessing the $p21^{WAF1}$, *Bax*, or *Mdm2* promoter regions were transfected into H1299 cells, together with or without increasing amounts of FLAG-LMO3 expression plasmid and a constant amount of p53. Enforced Plk1 expression was previously reported to inhibit the transcriptional activity of p53 [16] and therefore used to verify our results. As indicated in Fig. 2B,

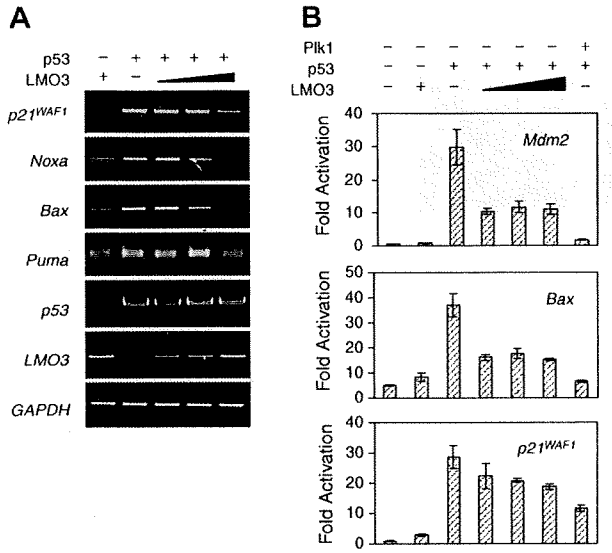

Fig. 2. LMO3 inhibits the transcriptional ability of p53. (A) mRNA levels of p53 target genes following p53 overexpression in p53-deficient H1299 cells, with co-expression of an increasing amount of LMO3 plasmid. Total RNA was extracted and subjected to RT-PCR analysis of *Noxa*, *Bax*, $p21^{WAF1}$ and *Puma*; detection of *GAPDH* was used as a loading control. (B) Luciferase gene reporter assay of $p21^{WAF1}$, *Bax* and *Mdm2* promoter regions. H1299 cells were transiently transfected with the indicated combination of p53 and increasing LMO3 plasmid. Results are the mean of three independent experiments ± standard deviation.

p53-mediated activation of $p21^{WAF1}$, *Bax*, and *Mdm2* promoter regions was reduced by co-expression of FLAG-LMO3 when compared to transfection of p53 alone. Therefore, both endogenous mRNA transcription and activation of p53-responsive promoter elements were reduced upon co-expression with LMO3. These findings signify that LMO3 acts as a co-repressor of p53, suppressing p53-mediated transcriptional regulation.

Promoter recruitment of p53 is affected by LMO3

We attempted to clarify the mechanism by which LMO3 represses p53-mediated gene activation. For this, we employed ChIP assays to characterize the recruitment of p53 onto p53-response elements in the *p21*, *Bax* and *Puma* promoters. Both p53 and LMO3 proteins could be expressed in H1299 cells, detected by western blot (Fig. 3A). This experimental system revealed that specific recruitment of exogenously expressed p53 onto the promoters of *p21*, *Bax*, and *Puma* genes in the presence or absence of HA-LMO3 (Fig. 3B). The specificity of the anti-p53 antibody to precipitate p53 bound chromatin is shown by the lack of PCR product in the absence of p53, LMO3 only transfection, and ChIP with normal mouse IgG. The effect of LMO3 on p53 recruitment to these regions appears to be promoter specific, as a clear increase in recruitment of p53 to the *p21* promoter was observed when LMO3 was present in cells. A similar tendency at *Bax* and *Puma* promoters was observed to a lesser extent.

Discussion

LMO3 can act as an oncogene by promoting cell survival when highly and abnormally expressed in neuroblastoma [14]. Furthermore, we report here that LMO3 inhibits p53, one of the key molecules in protection against cancer. This oncogenic action of LMO3 is comparable to the activity of other LIM-only protein family members against tumor suppressor proteins [19]. Additionally, the compensatory roles of LMO1 and LMO3 in development [6] suggest common mechanisms of activity between LIM-only proteins. Yet the timing of expression levels and topography result in subtly distinct outcomes. Taken together with our previous studies, recent results are consistent with the notion that LIM-only proteins are regulatory proteins which have essential functions in transcriptional regulation, while they can be potent oncogenes under conditions of abnormal expression.

We demonstrated that LMO3 represses p53-mediated activation and transcription of apoptosis-related genes. The loss of p53 activation provides tumor cells with several selective advantages, such as an increased tolerance to growth arrest and apoptosis-inducing protective mechanisms, in addition to genetic instability [3,5]. This indicates that p53 is either inactivated or repressed by LMO3, even though p53 still retains nuclear localization and DNA-binding capability. Additionally, activation of the DNA-damage response by CDDP treatment demonstrated a functioning p53 pathway in SH-SY5Y cells including the transcriptional activation of *p21* (Supplementary Fig. 1). Interestingly, p53 recruitment to the $p21^{WAF1}$ promoter was increased by LMO3 expression. However, in all p53-activated genes studied, LMO3 could repress their transcription by p53. Thus, LMO3 expression can influence p53 recruitment in a promoter selective manner but this may not be the main mechanism of repression.

As no enzymatic activity has been reported for LMO3, we propose that de-regulation of LMO3 expression leads to abnormal complex formation because of inappropriate LMO3 interactions. Our ChIP assay suggests that LMO3 does not suppress p53-mediated gene activation by interfering with DNA-binding. Therefore, another repression mechanism must exist. Accumulating evidence has demonstrated that post-translational modification of histones correlate with gene transcriptional regulation. Generally, Histone acetylation is associated with gene activation [20]. Physical and functional interactions of histone-acetyltransferases with p53, such as CBP and p300, demonstrate targeted acetylation of histones at promoter regions [21–23]. ChIP assays may indicate mod-

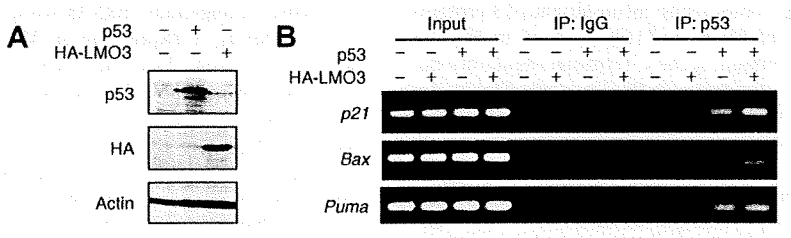

Fig. 3. Recruitment of p53 to promoters of apoptosis-related genes. (A) Immunoblotting showing expression of p53 and HA-LMO3 in p53-deficient H1299 cell line. (B) Chromatin immunoprecipitation with anti-p53 antibody or control mouse IgG in H1299 cells transfected with the indicated combinations of p53 and HA-LMO3 expression plasmids.

ification of histone acetylation by overexpression of LMO3 in the chromatin of p53-target genes. Future studies should examine the potential protein–protein interactions and the nature of LIM-only protein complexes involved in epigenetic modifications of chromatin.

The discrepancy between increased p53 recruitment and repression of gene activation could be explained by the following mechanisms. p53 receives a complex assortment of post-translational modifications including phosphorylation, ubiquitination, sumoylation, methylation and acetylation. These modifications affect many aspects of p53 status and activity, such as protein stability, DNA-binding activity, promoter selection and target-gene activation and/or repression. Regarding the repression of p53-mediated transcription by LMO3, we could not find any reduction in protein stability (data not shown) and DNA-binding activity of p53 to the *p21*, *bax*, and *puma* promoters. This suggests that LMO3 regulation of p53 may affect the association with its co-activators and repressors. It has been proposed that LIM-only proteins exert their effect by mediating protein–protein interactions and competing for interacting domains in the assembly of protein complexes [24,25]. Thus, LMO3 may directly compete for recruitment of negative transcriptional regulators to the p53 DNA-binding complex and promoter regions. Alternatively, LMO3 could recruit post-translational modifiers of p53 affecting transcriptional activation via an indirect mechanism. One other possibility, although not yet established for LIM-only proteins, is that binding by LMO3 affects the protein folding of p53, allowing recruitment to its response element yet interferes with assembly of the transcription machinery.

We expected that alterations in LMO3 transcriptional complexes have an inappropriate regulatory effect on downstream targets. Indeed, this is supported by our findings that the interaction of LMO3 with p53 represses p53-mediated transcription. This seems to be a common theme among LIM-only proteins. For example, LMO4 inhibits the transcriptional activity of BRCA1, a major tumor suppressor in breast cancers [10,19]. Intriguingly, Simonis et al. [26] found that *LMO3* is activated by chromosomal translocations of the T-cell receptor beta locus associated with T-cell lymphomas. In view of this study, the activities and molecular pathways of LMO3 activity identified here and in our previous report may be applicable to T-ALL. For future studies of LMO3, the regulation of gene expression itself needs to be clearly defined.

Long term survival, especially for those over 18 months of age for children with advanced neuroblastoma is currently unsatisfactory. Regardless of a myriad of treatments, recovery rates are poor. Present treatment regimes include surgery, radiation therapy, chemotherapy, retinoic acid and immunotherapy with anti-GD2 monoclonal antibody. Currently, in high risk groups (around half of all patients) overall survival is less than 40% [2]. There is an urgent necessity for specific therapies that can selectively eliminate cancer cells while limiting damage to normal cells and tissues. In particular, identification of novel targets and pathways through studies of abnormal gene expression, mutations, and genetic abnormalities in the various stages of neuroblastoma is crucial. Inhibition of LMO3 may be useful in treatment of presently difficult to treat neuroblastomas. The potential for interference of LIM-only protein multi-complexes and subsequent inhibition of normal and tumorigenic roles has been demonstrated using vector mediated expression of an anti-LMO2 single chain Fv antibody fragment [27,28]. Recent advances which will allow for individual gene profiling of tumors and the ability to design specific inhibitors may lead to a personalized treatment regime based on expression of individual oncogenes. Therefore, specific targeting of LMO3 in highly expressing tumors may simultaneously permit activation of the p53 pathway and inhibit LMO3-mediated pro-survival mechanisms.

Acknowledgments

This work was supported in part by a Grant-in-Aid from the Ministry of Health, Labour and Welfare for Third Term Comprehensive Control Research for Cancer, a Grant-in-Aid for Scientific Research on Priority Areas from the Ministry of Education, Culture, Sports, Science and Technology, Japan. A scholarship was awarded to S.L. from the Fujii medical foundation. The authors are grateful to Dr. Takehiko Kamijo for valuable discussion.

Appendix A. Supplementary data

Supplementary data associated with this article can be found, in the online version, at doi:10.1016/j.bbrc.2009.12.010.

References

[1] G.M. Brodeur, C. Azar, M. Brother, et al., Neuroblastoma. Effect of genetic factors on prognosis and treatment, Cancer 70 (1992) 1685–1694.
[2] J.M. Maris, M.D. Hogarty, R. Bagatell, et al., Neuroblastoma, Lancet 369 (2007) 2106–2120.
[3] B. Vogelstein, D. Lane, A.J. Levine, Surfing the p53 network, Nature 408 (2000) 307–310.
[4] J. Zhu, S. Zhang, J. Jiang, et al., Definition of the p53 functional domains necessary for inducing apoptosis, J. Biol. Chem. 275 (2000) 39927–39934.
[5] A.Y. Nikolaev, M. Li, N. Puskas, et al., Parc: a cytoplasmic anchor for p53, Cell 112 (2003) 29–40.
[6] E. Tse, A.J.H. Smith, S. Hunt, et al., Null mutation of the Lmo4 gene or a combined null mutation of the Lmo1/Lmo3 genes causes perinatal lethality, and Lmo4 controls neural tube development in mice, Mol. Cell. Biol. 24 (2004) 2063–2073.
[7] S. Arber, G. Halder, P. Caroni, Muscle LIM protein, a novel essential regulator of myogenesis, promotes myogenic differentiation, Cell 79 (1994) 221–231.
[8] T. Boehm, L. Foroni, Y. Kaneko, et al., The rhombotin family of cysteine-rich LIM-domain oncogenes: distinct members are involved in T-cell translocations to human chromosomes 11p15 and 11p13, Proc. Natl. Acad. Sci. USA 88 (1991) 4367–4371.
[9] Y. Yamada, A.J. Warren, C. Dobson, et al., The T cell leukemia LIM protein Lmo2 is necessary for adult mouse hematopoiesis, Proc. Natl. Acad. Sci. USA 95 (1998) 3890–3895.
[10] E.Y.M. Sum, D. Segara, B. Duscio, et al., Overexpression of LMO4 induces mammary hyperplasia, promotes cell invasion, and is a predictor of poor outcome in breast cancer, Proc. Natl. Acad. Sci. USA 102 (2005) 7659–7664.
[11] H. Mizunuma, J. Miyazawa, K. Sanada, et al., The LIM-only protein, LMO4, and the LIM domain-binding protein, LDB1, expression in squamous cell carcinomas of the oral cavity, Br. J. Cancer 88 (2003) 1543–1548.
[12] S. Mousses, L. Bubendorf, U. Wagner, et al., Clinical validation of candidate genes associated with prostate cancer progression in the CWR22 model system using tissue microarrays, Cancer Res. 62 (2002) 1256–1260.
[13] J. Bao, D.A. Talmage, L.W. Role, et al., Regulation of neurogenesis by interactions between HEN1 and neuronal LMO proteins, Development 127 (2000) 425–435.
[14] M. Aoyama, T. Ozaki, H. Inuzuka, et al., LMO3 interacts with neuronal transcription factor, HEN2, and acts as an oncogene in neuroblastoma, Cancer Res. 65 (2005) 4587–4597.
[15] M. Ohira, A. Morohashi, H. Inuzuka, et al., Expression profiling and characterization of 4200 genes cloned from primary neuroblastomas: identification of 305 genes differentially expressed between favorable and unfavorable subsets, Oncogene 22 (2003) 5525–5536.
[16] K. Ando, T. Ozaki, H. Yamamoto, et al., Polo-like kinase 1 (Plk1) inhibits p53 function by physical interaction and phosphorylation, J. Biol. Chem. 279 (2004) 25549–25561.
[17] N. Koida, T. Ozaki, H. Yamamoto, et al., Inhibitory role of Plk1 in the regulation of p73-dependent apoptosis through physical interaction and phosphorylation, J. Biol. Chem. 283 (2008) 8555–8563.
[18] H. Niizuma, Y. Nakamura, T. Ozaki, et al., Bcl-2 is a key regulator for the retinoic acid-induced apoptotic cell death in neuroblastoma, Oncogene 25 (2006) 5046–5055.
[19] E.Y.M. Sum, B. Peng, X. Yu, et al., The LIM domain protein LMO4 interacts with the cofactor CtIP and the tumor suppressor BRCA1 and inhibits BRCA1 activity, J. Biol. Chem. 277 (2002) 7849–7856.
[20] S.Y. Roth, J.M. Denu, C.D. Allis, Histone acetyltransferases, Annu. Rev. Biochem. 70 (2001) 81–120.
[21] N.A. Barlev, L. Liu, N.H. Chehab, et al., Acetylation of p53 activates transcription through recruitment of coactivators/histone acetyltransferases, Mol. Cell 8 (2001) 1243–1254.
[22] J.M. Espinosa, B.M. Emerson, Transcriptional regulation by p53 through intrinsic DNA/chromatin binding and site-directed cofactor recruitment, Mol. Cell 8 (2001) 57–69.
[23] W. An, J. Kim, R.G. Roeder, Ordered cooperative functions of PRMT1, p300, and CARM1 in transcriptional activation by p53, Cell 117 (2004) 735–748.

[24] J.L. Kadrmas, M.C. Beckerle, The LIM domain: from the cytoskeleton to the nucleus, Nat. Rev. Mol. Cell. Biol. 5 (2004) 920–931.
[25] H.P. Ostendorff, R.I. Peirano, M.A. Peters, et al., Ubiquitination-dependent cofactor exchange on LIM homeodomain transcription factors, Nature 416 (2002) 99–103.
[26] M. Simonis, P. Klous, I. Homminga, et al., High-resolution identification of balanced and complex chromosomal rearrangements by 4C technology, Nat. Methods 6 (2009) 837–842.
[27] C. Nam, M.N. Lobato, A. Appert, et al., An antibody inhibitor of the LMO2-protein complex blocks its normal and tumorigenic functions, Oncogene 27 (2008) 4962–4968.
[28] T. Tanaka, R.L. Williams, T.H. Rabbitts, Tumour prevention by a single antibody domain targeting the interaction of signal transduction proteins with RAS, EMBO J. 26 (2007) 3250–3259.

Imaging, Diagnosis, Prognosis

Clinical Cancer Research

Accurate Outcome Prediction in Neuroblastoma across Independent Data Sets Using a Multigene Signature

Katleen De Preter[1], Joëlle Vermeulen[1], Benedikt Brors[2], Olivier Delattre[4], Angelika Eggert[5], Matthias Fischer[6], Isabelle Janoueix-Lerosey[4], Cinzia Lavarino[7], John M. Maris[8], Jaume Mora[7], Akira Nakagawara[9], André Oberthuer[6], Miki Ohira[9], Gudrun Schleiermacher[4], Alexander Schramm[5], Johannes H. Schulte[5], Qun Wang[8], Frank Westermann[3], Frank Speleman[1], and Jo Vandesompele[1]

Abstract

Purpose: Reliable prognostic stratification remains a challenge for cancer patients, especially for diseases with variable clinical course such as neuroblastoma. Although numerous studies have shown that outcome might be predicted using gene expression signatures, independent cross-platform validation is often lacking.

Experimental Design: Using eight independent studies comprising 933 neuroblastoma patients, a prognostic gene expression classifier was developed, trained, tested, and validated. The classifier was established based on reanalysis of four published studies with updated clinical information, reannotation of the probe sequences, common risk definition for training cases, and a single method for gene selection (prediction analysis of microarray) and classification (correlation analysis).

Results: Based on 250 training samples from four published microarray data sets, a correlation signature was built using 42 robust prognostic genes. The resulting classifier was validated on 351 patients from four independent and unpublished data sets and on 129 remaining test samples from the published studies. Patients with divergent outcome in the total cohort, as well as in the different risk groups, were accurately classified (log-rank $P < 0.001$ for overall and progression-free survival in the four independent data sets). Moreover, the 42-gene classifier was shown to be an independent predictor for survival (odds ratio, >5).

Conclusion: The strength of this 42-gene classifier is its small number of genes and its cross-platform validity in which it outperforms other published prognostic signatures. The robustness and accuracy of the classifier enables prospective assessment of neuroblastoma patient outcome. Most importantly, this gene selection procedure might be an example for development and validation of robust gene expression signatures in other cancer entities. *Clin Cancer Res; 16(5); 1532–41. ©2010 AACR.*

One of the main challenges in clinical cancer research remains accurate prediction of outcome, enabling better choice of risk-related therapy. This is particularly true for neuroblastoma, a pediatric tumor of the sympathetic nervous system, which is characterized by a remarkably heterogeneous clinical course. Tumors that are found in infants frequently regress spontaneously or show differentiation features on treatment, whereas tumors diagnosed in children >1 year of age often metastasize, causing accelerated cancer-related death despite intensive therapies. Accordingly, different therapeutic schemes exist ranging from watch-and-see approaches to multimodal therapies. Four major risk stratification systems are currently being used in various parts of the world (Europe, United States, Japan, and Germany) based on a combination of clinicopathologic and genetic parameters, such as age at diagnosis, tumor stage, *MYCN* gene status, histopathologic classification, ploidy, and chromosome 1p and 11q status (1–8). Clinical experience within these systems indicates that the stratification is useful, but misclassifications occur, resulting in overtreatment or undertreatment. Identification of more specific and sensitive markers for response to therapy and outcome prediction is clearly required and is expected to result in better choice of risk-related therapy.

As differences in outcome are considered to reflect underlying genetic and biological characteristics that have

Authors' Affiliations: [1]Center for Medical Genetics, Ghent University, Ghent University Hospital, Ghent, Belgium; Departments of [2]Theoretical Bioinformatics and [3]Tumour Genetics, German Cancer Research Center, Heidelberg, Germany; [4]Institut National de la Sante et de la Recherche Medicale U830, Institut Curie, Paris, France; [5]Division of Hematology and Oncology, University Children's Hospital Essen, Essen, Germany; [6]Children's Hospital of Cologne, Department of Pediatric Oncology, Cologne, Germany; [7]Developmental Tumor Biology Laboratory, Hospital Sant Joan de Déu, Barcelona, Spain; [8]Division of Oncology, Children's Hospital of Philadelphia, University of Pennsylvania School of Medicine, Philadelphia, Pennsylvania; and [9]Division of Biochemistry, Chiba Cancer Center Research Institute, Chiba, Japan

Corresponding Author: Jo Vandesompele, Center for Medical Genetics, Ghent University Hospital, Medical Research Building, 2nd Floor, Room 120.055, De Pintelaan 185, B-9000 Ghent, Belgium. Phone: 32-9-332-5187; Fax: 32-9-332-6549; E-mail: Joke.Vandesompele@UGent.be.

doi: 10.1158/1078-0432.CCR-09-2607

Translational Relevance

Prognostic classification of heterogeneous diseases such as neuroblastoma remains challenging. In this study, a unique data-mining approach was applied for establishment of an accurate and robust gene expression classifier to predict clinical outcome of neuroblastoma patients. Using both published and unpublished microarray expression data of 933 primary neuroblastomas, a 42-gene classifier was developed and successfully validated. The powerful and independent prognostic value of the 42-gene classifier is shown using several lines of evidence. First, patients with divergent outcome were accurately classified. Second, multivariate analysis showed that the classifier is an independent prognostic factor, contributing to more accurate assessment of prognosis when considering the conventional risk factors alone. This was further confirmed within a subgroup of high-risk patients. Moreover, the excellent performance of the classifier across different expression platforms clearly shows its robustness. The presented gene selection procedure is suitable for the development of gene expression signatures in other cancer entities.

their effect on mRNA gene expression profiles, several microarray expression profiling studies have been undertaken to predict patient outcome in different cancer entities.

An important limitation of many published gene expression profiling studies is the lack of statistical power to identify markers and lack of independent validation. Typically, around 30,000 to 40,000 transcripts are tested, generating hundreds of thousands of data points for a relatively small subset of tumors (between 20 and 100). When such a high number of genes are evaluated as prognostic markers, there is a substantial chance that a random association between a gene and the prognostic classes is observed (9, 10). Consequently, many published studies do not classify patients better than chance due to lack of internal validation by repeated random sampling of training sets or external validation on independent samples. As such, there are a few inherent but often overlooked statistical issues, such as data overfitting, unstable gene lists, and lack of study power (11).

In this study, we established a prognostic 42-gene classifier for children with neuroblastoma by reanalysis of four published gene expression studies from four different microarray platforms comprising 582 patients in total (12–15). To facilitate data comparison across different platforms, probe annotations were updated with respect to the original publications. When available, clinical follow-up information was updated. All these aspects critically contribute to the success of our multigene signature. Successful validation of the multigene signature in four independent unpublished data sets shows its robust performance and platform independence.

Materials and Methods

Gene expression data sets. Four published studies were used for selecting the genes and building the prognostic classifier (phase 1 data sets), and four unpublished data sets were used as independent validation sets (phase 2 data sets).

The phase 1 data sets were downloaded either from the National Center for Biotechnology Information Gene Expression Omnibus (GSE2283 and GSE3960; refs. 14, 15) or from the European Bioinformatics Institute ArrayExpress database (E-TABM-38; ref. 13), or from the authors' Web site[10] (12).

A trained multigene correlation signature was validated on the four independent phase 2 data sets from which the 42 genes (when present) were extracted and standardized (per gene, the median value across the samples was subtracted followed by division by the SD of the gene): (*a*) hgu95av2 Affymetrix gene expression data from 106 neuroblastoma patients (validation set 1; 40 genes present), (*b*) hgu133plus2 Affymetrix gene expression data from 53 neuroblastoma patients (validation set 2; 40 genes present), (*c*) data set for 91 neuroblastoma patients obtained using an 11K custom Agilent oligonucleotide microarray (validation set 3; 41 genes present), and (*d*) Human Exon 1.0 ST Affymetrix expression data from 101 neuroblastoma patients (validation set 4; 42 genes present; standardized data of the 42-gene selection as well as clinical data are available in Supplementary Tables S1 and S2; Fig. 1).

For the remainder of the article, we will label the data sets according to the first author for the published phase 1 studies [Oberthuer (13), Wang (15), Berwanger (12), and Ohira (14)] and as validation sets 1, 2, 3, and 4 for the unpublished phase 2 studies.

Data preprocessing. To make the data from the different microarray platforms maximally comparable, annotation information of the probes was updated using the MatchMiner tool (16) for the custom-made cDNA or oligonucleotide arrays (12–14) and using the latest version of the R packages hgu95av2 and hgu133plus2 for the Affymetrix array data (15). Probe identification numbers were converted into gene symbols to enable straightforward comparison of the gene lists between the different studies. Throughout the text, the number of unique gene symbols (represented by one or more array probes) in each study is indicated.

Updated clinical information with regard to progression-free survival (PFS) and overall survival (OS) times was obtained from the authors (14, 15) or was publicly available (13). For the Berwanger and Ohira studies and validation set 1, only OS data were available.

[10] http://www.imt.uni-marburg.de/microarray/download.html

Patients were divided in two clearly defined risk groups. The low-risk subgroup was defined by stage I, II, or IVS without *MYCN* amplification, and the high-risk subgroup comprised patients with age of diagnosis >1 y with stage IV tumors (irrespective of *MYCN* status) or with stage II and III tumors with *MYCN* amplification. To develop our classifier, as many patients as possible from the four phase 1 data sets were divided in the two risk groups with maximally divergent clinical course (Table 1), that is, low-risk patients with PFS time (or OS time for Berwanger and Ohira data sets) of at least 1,000 d and high-risk patients that died from the disease. The patients that did not belong to the above-mentioned low- or high-risk subgroups were used as independent test set.

Statistical analysis. Identification and validation of prognostic classifiers (for each single phase 1 data set) were done by prediction analysis of microarray (PAM) classification with 10-times repeated 10-fold cross-validation in

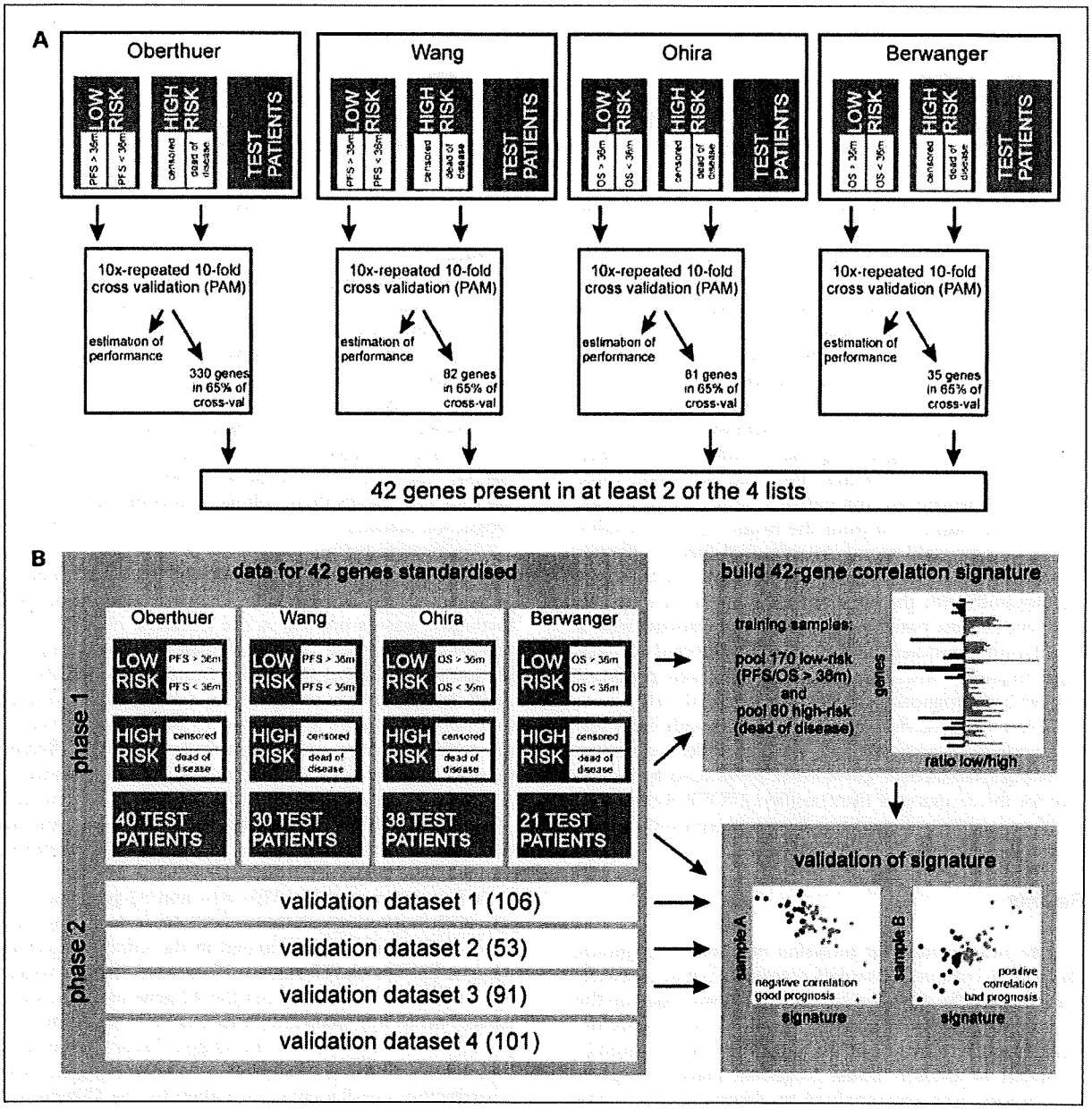

Fig. 1. Outline of the strategy used for prioritization of the 42 prognostic gene list (A) and construction of a 42-gene correlation signature and validation on independent test samples from phase 1 studies and phase 2 validation data sets (B). m, months.

Table 1. Published phase 1 studies used for training the classifier, with indication of the number of (training) samples, median OS or PFS (in months), and estimation of the performance of the study-specific PAM classifier for prediction of unfavorable outcome (OS)

	Berwanger	Oberthuer	Ohira	Wang
No. patients	94	251	136	101
No. low-risk training samples	22	87	43	18
No. high-risk training samples	13	25	20	22
Median OS/PFS (mo)	OS = 43	PFS = 55	OS = 46	PFS = 48
Specificity	0.955	0.977	0.814	1.000
Sensitivity	1.000	0.960	0.950	0.773
Negative predictive value	0.929	0.923	0.704	1.000
Positive predictive value	1.000	0.988	0.972	0.783
Accuracy	0.971	0.973	0.857	0.875
Performance (AUC)	0.977	0.969	0.882	0.886

the R statistical language using the Bioconductor package MCRestimate (Fig. 1A; refs. 13, 17). Forty-two genes were present in at least two of the four resulting gene lists.

A cross-platform gene signature was built using standardized expression data of the 42 genes (if present on the respective arrays, see Supplementary Data 2) from four published phase 1 studies. The correlation method was used to build and test a cross-platform prognostic signature (Fig. 1B). Log-transformed data were merged in one file (if more than one probe was present for a certain gene, the probe with the highest expression value was selected), and for each of the 42 genes, the mean expression value in low-risk neuroblastoma patients with PFS of at least 1,000 d was subtracted from the mean expression value in high-risk neuroblastoma patients that died of disease. For classification, the Pearson's correlation coefficient of the signature with the standardized expression values of independent test patients was calculated. Patients with a correlation coefficient below 0 were predicted to have good prognosis, whereas the other patients were predicted to have bad prognosis [according to Liu et al. (18)].

Kaplan-Meier survival analysis was done with the R survival package (R version 2.6.1). The area under the receiver operating characteristic curve (AUC) was used as a measure for the accuracy of the classifiers (ROCR R-package). Multivariate forward conditional logistic regression analysis was done using SPSS version 16.

Results

Gene prioritization for inclusion in a robust prognostic classifier. A complete 10-times repeated 10-fold cross-validation using the PAM algorithm (13, 19) was done on the training patients belonging to one of the two clearly defined risk groups from the four published phase 1 studies separately to identify robust prognostic markers (Fig. 1). This process was accompanied by determination of the classification accuracy, providing a first estimation of the utility of the expression data to predict outcome (Table 1).

For each data set, we selected the probes that were included in at least 65 of the 100 cross-validation gene lists, as these genes are likely to be the ones with the highest prognostic value as determined by Oberthuer et al. (13). The resulting prognostic gene lists from the four studies showed significant overlap (Table 2; Supplementary Data 1). Two genes were in common between three lists (i.e., *MYCN* and *NTRK1*), whereas 40 genes were in common between two lists. Thirty-two were previously reported in at least 1 of 10 published prognostic gene lists, of which only 10 were found in 2 or more published prognostic lists (12–14, 20–26). The occurrence of the 42 genes in at least two of the four lists makes them robust, platform-independent, prognostic markers.

Classification performance of the 42-gene list. Next, we investigated whether the 42-gene list is able to predict prognosis across different data sets. The classification performance was estimated in the different phase 1 data sets using a complete 10-times repeated 10-fold cross-validation method using all patients from the two clearly defined risk groups. For this analysis, it is important to note that not all 42 genes are present on all platforms; hence, the performance test was inherently done with a different number of genes for the different data sets (Supplementary Data 2). As already indicated, the 10-times repeated 10-fold cross-validation provides a good estimate for the classification performance using the expression data of the selected gene list.

As a reference, the 35-, 330-, 81-, and 82-gene lists obtained through single PAM analysis of each of the four phase 1 data sets were evaluated in the same way as the 42-gene list. The classification performance was also tested for a subset of 11 genes (from the 42-gene list) that were present on all four platforms. This analysis showed that all performance parameters for the 42-gene list are best or second best for all studies compared with the other gene lists, whereby the overall accuracy is highest for the 42-gene list subset (AUC = 0.935; Supplementary Data 2). This analysis also shows that the performance of a classifier built for

a given data set is not always best, which indicates the power and utility of our meta-analysis for the identification of a prognostic gene list by using expression data of 250 training samples (170 low risk and 80 high risk). When only 11 genes of the 42-gene list were selected that are present on all four platforms, the overall accuracy was lower due to loss in sensitivity and positive predictive value. The 42-gene classifier was also compared with two published classifiers (13, 27) and showed that the 42-gene classifier performs best.

Table 2. Genes that are in common between the 42-gene list and the different individual classifier gene lists (number of common genes in list/total number of genes in list)

	Berwanger (10/35)	Oberthuer (38/330)	Ohira (12/81)	Wang (26/82)	published lists
AHCY		–	–		2
AKR1C1		+		+	1
ARHGEF7		+	+		2
BIRC5	–		–		1
CADM1		+		+	0
CAMTA2		+		+	0
CDCA5	–	–			2
CDKN3		–		–	2
CLSTN1		+		+	1
DDC		+	+		1
DPYSL3		+	+		1
ECEL1		+	+		0
EPB41L3		+		+	0
EPHA5	+	+			1
EPN2		+		+	0
FYN			+	+	1
GNB1		+	+		1
HIVEP2		+		+	1
INPP1	+			+	1
MAP7	+	+			1
MAPT		+	+		1
MCM2		–		–	0
MRPL3		–		–	1
MYCN	–	–	–		4
NCAN		–		–	0
NME1	–	–			2
NRCAM		+		+	2
NTRK1		+	+	+	4
ODC1	–			–	1
PAICS		–		–	1
PLAGL1	+	+			1
PMP22		+		+	1
PRKACB		+		+	2
PRKCZ		+		+	1
PTN		+		+	1
PTPRN2		+	+		0
SCG2		+		+	1
SLC25A5		–		–	1
SNAPC1		–		–	0
TYMS		–		–	1
ULK2		+		+	0
WSB1	+	+			4

NOTE: The number of published prognostic gene lists (other than the four reanalyzed studies) in which these genes are found is indicated in the last column. –, associated with poor outcome; +, associated with favorable outcome.

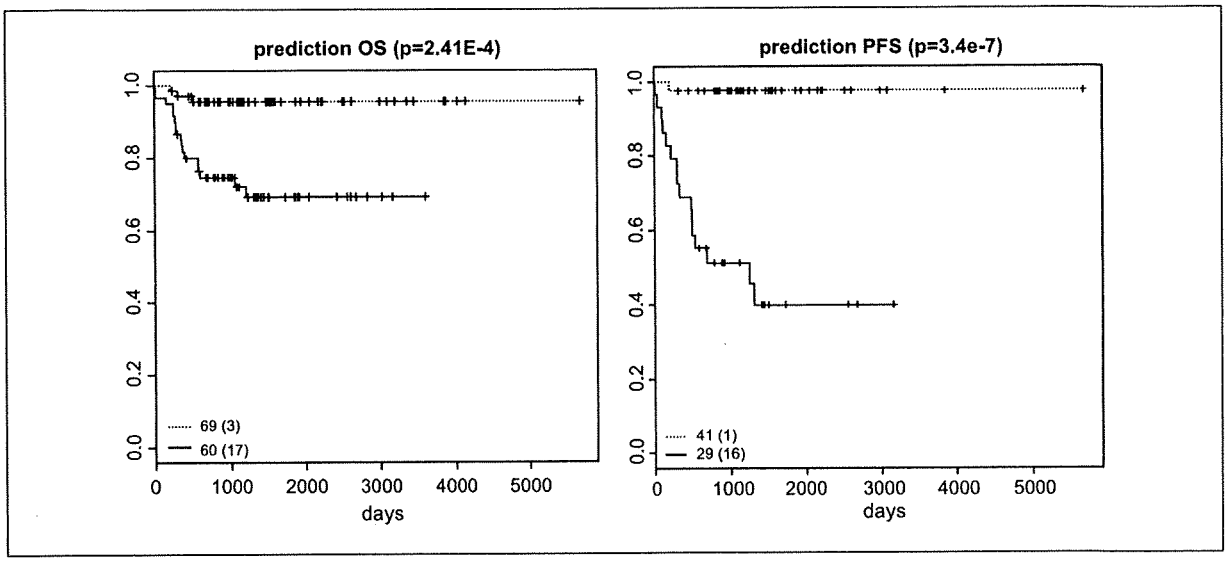

Fig. 2. Kaplan-Meier and log-rank analysis of 129 test patients (OS) and 70 test patients (PFS) from the four published phase 1 studies classified using the prognostic correlation signature. Legend, number of patients in predicted subgroups; between brackets, number of patients with event (relapse, progression, or death).

Validation of a cross-platform prognostic 42-gene correlation signature for neuroblastoma. A major disadvantage of the PAM classification method is the need for a training set of samples that are analyzed on the same gene expression measurement platform as the one used to evaluate the test samples. We therefore applied an alternative method to build a classifier based on the 42-gene list that can be used for completely independent data sets even on other platforms.

The prognostic signature is determined using 250 training samples from the four phase 1 studies. A 42-gene classification vector was created and tested using the correlation method (see Materials and Methods; Fig. 1).

First, the correlation signature was tested on the 129 test samples (patients not belonging to the low- and high-risk subgroup) from the four phase 1 studies and revealed a very high predictive power for OS (log-rank P = 2.41E–4) and PFS (log-rank P = 3.40E–7; Fig. 2).

Next, this correlation signature was evaluated on the four independent phase 2 data sets (351 patients), whereby the patients could be clearly separated into groups with significant differences in OS (log-rank P = 2.17E–23) and PFS (log-rank P = 2.03E–21; Fig. 3A). Kaplan-Meier analysis of patients stratified using known risk factors (i.e., age, stage, and *MYCN* gene status) showed that the correlation signature outperforms these risk factors ($P < 0.001$, except for *MYCN*-amplified samples; Supplementary Fig. S2). This was confirmed using multivariate logistic regression analysis evaluating age, stage, *MYCN* status, and the gene classifier, indicating that the 42-gene signature is an independent predictor for PFS and OS in the four phase 2 data sets as well as in the test samples of the phase 1 data sets (Table 3). Of note, whereas phase 2 data sets are representative of the general neuroblastoma population, test samples from the phase 1 data sets only represent intermediate risk patients.

As the different validation data sets include patients stratified using different risk stratification systems (Europe, United States, and Germany), we defined a common low- and high-risk group (Supplementary Data 3). As there was only 1 patient of 50 that died of disease within the common low-risk group of patients, we did not do Kaplan-Meier analysis. However, we could show that this single patient was classified in the high-molecular risk group using our classifier. Most interestingly, the correlation signature could partition patients within the common high-risk subgroup into groups with significant differences in OS and PFS (Fig. 3B) and was an independent prognostic marker (odds ratios, >4; Supplementary Table S4). To exclude that the significant survival differences in high-risk tumors is solely due to the effect of the *MYCN* amplification and related downstream *MYCN* signaling, we also tested the survival in high-risk tumors without *MYCN* amplification and could show that the classifier also significantly discriminates these patients with respect to outcome (Fig. 3C; Supplementary Table S4). In line with this, inspection of the 42-gene list indicated that not all 42-genes are related to *MYCN* amplification (Supplementary Data 4).

Discussion

In this study, we developed and validated a 42-gene prognostic classifier for children with neuroblastoma through a reanalysis strategy of published data complemented with gene expression data from 351 patients from

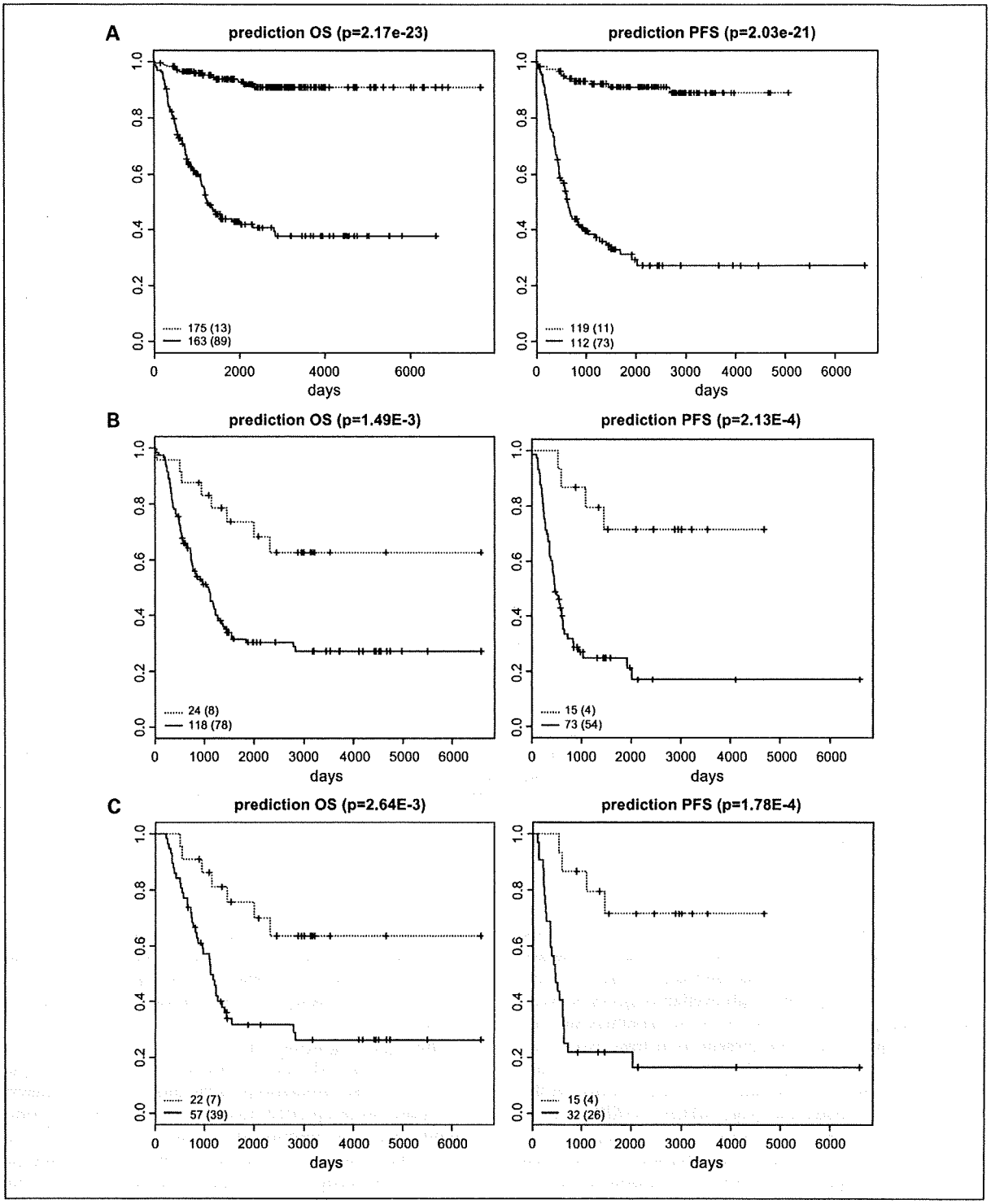

Fig. 3. Kaplan-Meier and log-rank analysis of the patients from four independent unpublished phase 2 validation data sets classified using the prognostic correlation signature for all patients together {5-y OS of 93.9% [95% confidence interval (95% CI), 90.2-97.6] for low molecular risk versus 43.1% (95% CI, 35.6-52.2) for high molecular risk and 5-y PFS of 91.1% (95% CI, 86.0-96.6) for low molecular risk versus 30.4% (95% CI, 22.1-41.8) for high molecular risk; A}, for the common high-risk subgroup (B), and for the common high-risk subgroup without MYCN amplification (C). Legend, number of patients in predicted subgroups; between brackets, number of patients with event (relapse, progression, or death).

Table 3. Multivariate logistic regression analysis (with correlation signature classification, MYCN status, International Neuroblastoma Staging System stage, and age at diagnosis; A) and sensitivity, specificity, and accuracy (AUC with 95% CI) results (follow-up time of at least 36 mo; B) for correlation signature prediction in the independent test samples from the phase 1 data sets and in the phase 2 validation data sets

A

		OS		PFS	
		P	OR (95% CI)	*P*	OR (95% CI)
Test samples from phase 1 data sets	Correlation signature	3.16E–2	5.11 (1.16-22.58)	3.12E–4	54.00 (6.17-472.41)
	MYCN amplification	7.80E–5	21.50 (4.69-98.54)	1.26E–1	—
	Stage (IV versus other)	1.80E–1	—	2.65E–1	—
	age (<1 or >1 y)	1.52E–1	—	8.65E–1	—
Phase 2 validation data sets	Correlation signature	9.07E–7	7.02 (3.23-15.28)	1.1E–14	16.45 (8.09-33.48)
	MYCN amplification	4.19E–2	2.23 (1.03-4.84)	3.13E–1	—
	Stage (IV versus other)	1.35E–2	2.50 (1.21-5.16)	2.16E–1	—
	age (<1 or >1 y)	1.45E–4	4.14 (1.99-3.66)	1.1E–4	4.18 (2.03-8.64)

B

	Test samples from phase 1 data sets	Phase 2 validation data sets
Sensitivity OS	17/20 = 0.85	89/102 = 0.87
Specificity OS	41/67 = 0.61	140/195 = 0.72
Performance, AUC (95% CI), OS	0.731 (0.612-0.850)	0.795 (0.742-0.849)
Sensitivity PFS	16/17 = 0.94	93/110 = 0.85
Specificity PFS	27/35 = 0.77	95/119 = 0.80
Performance, AUC (95% CI), PFS	0.856 (0.748-0.964)	0.822 (0.764-0.879)

NOTE: —, not analyzed.
Abbreviation: OR, odds ratio.

four unpublished data sets (Fig. 1). To accomplish this, four published microarray studies comprising >500 neuroblastoma patients were reanalyzed generating four new prognostic gene lists with a high overlap of genes between them. Comparison of the genes in the classifiers showed that 42 unique genes were present in at least two of the four lists. Not surprisingly, this set of 42 predictor genes contains numerous genes that have been reported in the context of neuroblastoma (e.g., *MYCN*, *NTRK1*, *NME1*, *CADM1*, *FYN*, *ODC1*, and *WSB1*). The finding of these genes in at least two independent studies indicates their robustness as prognostic markers. Comparison of the performance of the 42-gene list with the lists that were generated on the individual phase 1 studies and with two published prognostic gene lists (13, 27) showed that the classifier based on the 42-gene list has the highest overall accuracy while using the lowest number of genes. However, we have to keep in mind that this observed superiority of the 42-gene set might in part be due to the fact that, for some of the other gene lists, a large proportion of genes were not present on the platform (Supplementary Table S3).

The high prognostic classification performance of the 42-gene list is undoubtedly due to our unique reanalysis approach. First, annotations of the probes on the different platforms were updated according to the latest genome build. Second, a uniform risk definition was applied to select training patients across the different studies. Only patients with maximally divergent courses were used for training. Third, the same powerful algorithm with built-in cross-validation was used for identification of prognostic genes in four major published data sets, enabling the generation of relatively stable prognostic gene lists with high overlap.

This list of 42 prognostic genes was used to build a cross-platform classification signature. As the PAM algorithm is not suitable for cross-platform classification, we used a more intuitive, alternative method for building a 42-gene classifier. In this study, we generated a prognostic correlation signature based on expression data of the 42 genes in 250 training samples of the four phase 1 data sets. The signature was subsequently applied on independent test samples from the phase 1 data sets and on four independent and unpublished phase 2 data sets, generated on different expression profiling platforms, totaling 480 patients. The excellent prognostic performance of the 42-gene list (Table 3) further shows the validity of our meta-analysis approach and the utility of the recognized prognostic markers for neuroblastoma. The classifier predicts overall (OS) and PFS for the patients from the four phase 2 studies as well as for the test patients from the phase 1 studies (which could not be unequivocally classified in the low- or high-risk subgroups using known risk factors) with high sensitivity and specificity (Table 3). Importantly, the classifier was shown to be an independent predictor for both PFS and OS when stratifying for known risk factors such as age, stage, and *MYCN* status. Indeed, the 42-gene list does not only contain *MYCN*-regulated genes and, thus, not only reflects the *MYCN* copy number status of the samples. This is further substantiated by the excellent performance of the classifier in the high-risk neuroblastoma patients without *MYCN* amplification.

Thus far, this is the largest prognostic meta-analysis study in neuroblastoma, totaling >900 patients, including 351 patients from four independent and unpublished validation data sets. In contrast to other studies on neuroblastoma gene expression classifiers (13, 14, 21, 25, 27, 28), we could show an excellent performance of our classifier on these four independent data sets involving patients from different risk protocols from Germany, Europe, and United States by using a smaller gene set and a more intuitive classification method.

This survival classifier will definitely help to identify patients with increased risk in the current risk groups and to make a better choice of risk-related therapy. For example, low-risk patients with high molecular risk might benefit from more aggressive treatment protocols, whereas more intensive follow-up and new experimental therapies might be considered for high-risk patients with high molecular risk.

In conclusion, we applied a unique meta-analysis strategy for the identification of a robust set of 42 prognostic genes for outcome prediction in neuroblastoma. Furthermore, we propose a prognostic gene signature that is significantly associated with outcome prediction in neuroblastoma samples from independent studies using different technological platforms, making it a useful and practical classifier for risk stratification in neuroblastoma patients. The signature remains to be tested in a prospective clinical validation. The low number of genes makes this signature very well suited for cost-effective and fast PCR-based analysis, requiring only minimal amounts of tumor material, as exemplified by a recently published quantitative PCR study in which a 59-gene classifier containing the 42 genes from this study was trained, tested, and independently validated on a large cohort of patients (29). The outlined strategy for robust selection of prognostic markers and the use of a cross-platform correlation signature have wide application potential in other cancer entities.

In the search of an optimal prognostic classifier, it could prove useful to do an integrated analysis to determine the combined prognostic power of a mRNA gene expression signature along with gene copy number levels, microRNA gene expression patterns, and epigenetic modifications.

Disclosure of Potential Conflicts of Interest

No potential conflicts of interest were disclosed.

Acknowledgments

We thank Vincent Detours for critical reading of the manuscript and helpful suggestions and the Children's Oncology group.

Grant Support

European Community under the FP6 (project: STREP: EET-pipeline, number: 037260). This article presents research results of the Belgian program of Interuniversity Poles of Attraction, initiated by the Belgian State, Prime Minister's Office, Science Policy Programming. K. De Preter is a postdoctoral researcher with the Fund for Scientific Research-Flanders. J. Vermeulen is a Ph.D. student with the Belgian Kid's Fund and the Fondation pour la recherche Nuovo-Soldati. This study was sponsored by the 'Kinderkankerfonds,' the 'Stichting tegen Kanker,' the Fund for Scientific Research and BOF-UGent, and the fondation Fournier Majoie pour l'innovation.

The costs of publication of this article were defrayed in part by the payment of page charges. This article must therefore be hereby marked *advertisement* in accordance with 18 U.S.C. Section 1734 solely to indicate this fact.

Received 09/27/2009; revised 11/27/2009; accepted 12/22/2009; published OnlineFirst 02/23/2010.

References

1. Brodeur GM, Fong CT, Morita M, Griffith R, Hayes FA, Seeger RC. Molecular analysis and clinical significance of N-myc amplification and chromosome 1p monosomy in human neuroblastomas. Prog Clin Biol Res 1988;271:3–15.
2. Brodeur GM, Pritchard J, Berthold F, et al. Revisions of the international criteria for neuroblastoma diagnosis, staging, and response to treatment. J Clin Oncol 1993;11:1466–77.
3. Brodeur GM, Seeger RC, Schwab M, Varmus HE, Bishop JM. Amplification of N-myc in untreated human neuroblastomas correlates with advanced disease stage. Science 1984;224:1121–4.
4. Evans AE, D'Angio GJ, Randolph J. A proposed staging for children with neuroblastoma. Children's cancer study group A. Cancer 1971; 27:374–8.
5. Look AT, Hayes FA, Nitschke R, McWilliams NB, Green AA. Cellular DNA content as a predictor of response to chemotherapy in infants with unresectable neuroblastoma. N Engl J Med 1984;311:231–5.

6. Maris JM. The biologic basis for neuroblastoma heterogeneity and risk stratification. Curr Opin Pediatr 2005;17:7–13.
7. Shimada H, Ambros IM, Dehner LP, et al. The International Neuroblastoma Pathology Classification (the Shimada system). Cancer 1999;86:364–72.
8. Cohn SL, Pearson AD, London WB, et al. The International Neuroblastoma Risk Group (INRG) classification system: an INRG Task Force report. J Clin Oncol 2009;27:289–97.
9. Simon R. Diagnostic and prognostic prediction using gene expression profiles in high-dimensional microarray data. Br J Cancer 2003; 89:1599–604.
10. Tinker AV, Boussioutas A, Bowtell DD. The challenges of gene expression microarrays for the study of human cancer. Cancer Cell 2006;9:333–9.
11. Michiels S, Koscielny S, Hill C. Prediction of cancer outcome with microarrays: a multiple random validation strategy. Lancet 2005; 365:488–92.
12. Berwanger B, Hartmann O, Bergmann E, et al. Loss of a FYN-regulated differentiation and growth arrest pathway in advanced stage neuroblastoma. Cancer Cell 2002;2:377–86.
13. Oberthuer A, Berthold F, Warnat P, et al. Customized oligonucleotide microarray gene expression-based classification of neuroblastoma patients outperforms current clinical risk stratification. J Clin Oncol 2006;24:5070–8.
14. Ohira M, Oba S, Nakamura Y, et al. Expression profiling using a tumor-specific cDNA microarray predicts the prognosis of intermediate risk neuroblastomas. Cancer Cell 2005;7:337–50.
15. Wang Q, Diskin S, Rappaport E, et al. Integrative genomics identifies distinct molecular classes of neuroblastoma and shows that multiple genes are targeted by regional alterations in DNA copy number. Cancer Res 2006;66:6050–62.
16. Bussey KJ, Kane D, Sunshine M, et al. MatchMiner: a tool for batch navigation among gene and gene product identifiers. Genome Biol 2003;4:R27.
17. Ruschhaupt M, Huber W, Poustka A, Mansmann U. A compendium to ensure computational reproducibility in high-dimensional classification tasks. Stat Appl Genet Mol Biol 2004;3:Article37.
18. Liu R, Wang X, Chen GY, et al. The prognostic role of a gene signature from tumorigenic breast-cancer cells. N Engl J Med 2007;356:217–26.
19. Tibshirani R, Hastie T, Narasimhan B, Chu G. Diagnosis of multiple cancer types by shrunken centroids of gene expression. Proc Natl Acad Sci U S A 2002;99:6567–72.
20. Yamanaka Y, Hamazaki Y, Sato Y, et al. Maturational sequence of neuroblastoma revealed by molecular analysis on cDNA microarrays. Int J Oncol 2002;21:803–7.
21. Wei JS, Greer BT, Westermann F, et al. Prediction of clinical outcome using gene expression profiling and artificial neural networks for patients with neuroblastoma. Cancer Res 2004;64: 6883–91.
22. Takita J, Ishii M, Tsutsumi S, et al. Gene expression profiling and identification of novel prognostic marker genes in neuroblastoma. Genes Chromosomes Cancer 2004;40:120–32.
23. Ohira M, Morohashi A, Inuzuka H, et al. Expression profiling and characterization of 4200 genes cloned from primary neuroblastomas: identification of 305 genes differentially expressed between favorable and unfavorable subsets. Oncogene 2003;22: 5525–36.
24. Hiyama E, Hiyama K, Yamaoka H, Sueda T, Reynolds CP, Yokoyama T. Expression profiling of favorable and unfavorable neuroblastomas. Pediatr Surg Int 2004;20:33–8.
25. Asgharzadeh S, Pique-Regi R, Sposto R, et al. Prognostic significance of gene expression profiles of metastatic neuroblastomas lacking MYCN gene amplification. J Natl Cancer Inst 2006;98: 1193–203.
26. Abel F, Sjoberg RM, Nilsson S, Kogner P, Martinsson T. Imbalance of the mitochondrial pro- and anti-apoptotic mediators in neuroblastoma tumours with unfavourable biology. Eur J Cancer 2005; 41:635–46.
27. Chen QR, Song YK, Wei JS, et al. An integrated cross-platform prognosis study on neuroblastoma patients. Genomics 2008;92: 195–203.
28. Warnat P, Oberthuer A, Fischer M, Westermann F, Eils R, Brors B. Cross-study analysis of gene expression data for intermediate neuroblastoma identifies two biological subtypes. BMC Cancer 2007;7:89.
29. Vermeulen J, De Preter K, Naranjo A, et al. Predicting outcomes for children with neuroblastoma using a multigene-expression signature: a retrospective SIOPEN/COG/GPOH study. Lancet Oncol 2009;10: 663–71.